

## Photoluminescence studies of type-II diluted magnetic semiconductor Zn Mn Te Zn Se quantum dots

M. C. Kuo, J. S. Hsu, J. L. Shen, K. C. Chiu, W. C. Fan, Y. C. Lin, C. H. Chia, W. C. Chou, M. Yasar, R. Mallory, A. Petrou, and H. Luo

Citation: *Applied Physics Letters* **89**, 263111 (2006); doi: 10.1063/1.2424654

View online: <http://dx.doi.org/10.1063/1.2424654>

View Table of Contents: <http://scitation.aip.org/content/aip/journal/apl/89/26?ver=pdfcov>

Published by the [AIP Publishing](#)

---

### Articles you may be interested in

[Electric field control of magnetization dynamics in Zn Mn Se Zn Be Se diluted-magnetic-semiconductor heterostructures](#)

*Appl. Phys. Lett.* **88**, 212105 (2006); 10.1063/1.2206681

[Semimagnetic self-organized Cd 1x Mn x Te quantum dots generated by postgrowth thermal annealing](#)

*Appl. Phys. Lett.* **78**, 2140 (2001); 10.1063/1.1362199

[Magneto-optical mode conversion in Cd 1x Mn x Te waveguide on GaAs substrate](#)

*Appl. Phys. Lett.* **77**, 1593 (2000); 10.1063/1.1310176

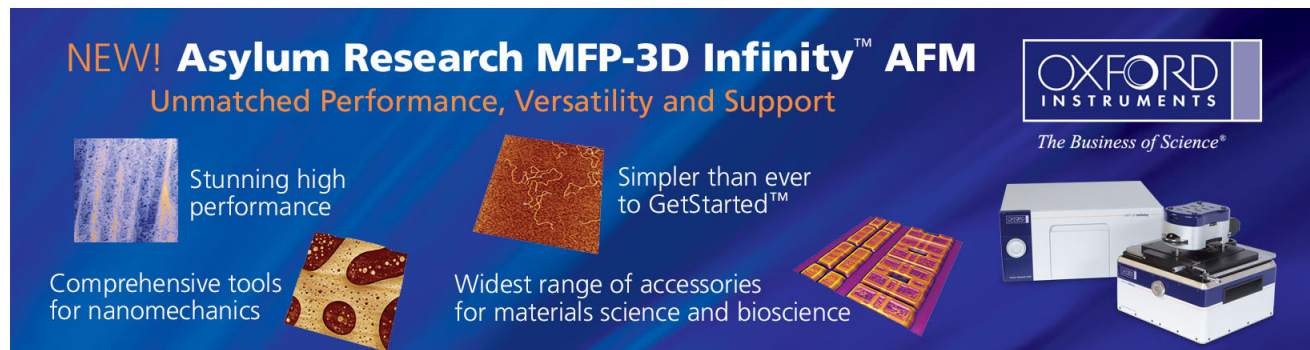
[Self-organized formation and photoluminescence of Cd 1x Mn x Te quantum dots grown on ZnTe by atomic layer epitaxy](#)

*Appl. Phys. Lett.* **76**, 2400 (2000); 10.1063/1.126357

[Time-resolved magneto-optical experiments in Cd 1x Mn x Te/ZnTe multiple quantum wells](#)

*J. Appl. Phys.* **85**, 5938 (1999); 10.1063/1.369997

---

An advertisement for the Asylum Research MFP-3D Infinity AFM. The background is dark blue. At the top left, the text reads 'NEW! Asylum Research MFP-3D Infinity™ AFM' in white and orange, followed by 'Unmatched Performance, Versatility and Support' in orange. On the right is the Oxford Instruments logo with the tagline 'The Business of Science®'. Below the text are four images: a blue textured surface, a brown textured surface, a grid of yellow and red squares, and the physical AFM instrument. Text descriptions are placed around these images: 'Stunning high performance' (top left), 'Simpler than ever to GetStarted™' (top right), 'Comprehensive tools for nanomechanics' (bottom left), and 'Widest range of accessories for materials science and bioscience' (bottom right).

## Photoluminescence studies of type-II diluted magnetic semiconductor ZnMnTe/ZnSe quantum dots

M. C. Kuo, J. S. Hsu, J. L. Shen, and K. C. Chiu

*Department of Physics, Chung Yuan Christian University, Chung-Li 32023, Taiwan, Republic of China*

W. C. Fan, Y. C. Lin, C. H. Chia, and W. C. Chou<sup>a)</sup>

*Department of Electrophysics, National Chiao Tung University, HsinChu 30010, Taiwan, Republic of China*

M. Yasar, R. Mallory, A. Petrou, and H. Luo

*Department of Physics, State University of New York at Buffalo, Buffalo, New York 14260*

(Received 9 August 2006; accepted 28 November 2006; published online 28 December 2006)

Type-II diluted magnetic semiconductor ZnMnTe quantum dots (QDs) in ZnSe matrix grown by molecular beam epitaxy were investigated by conventional and magnetophotoluminescence (PL) spectroscopy. The QD emission exhibits a type-II characteristic in excitation power dependence of PL peak energy. A nonzero circular polarization of PL at the absence of magnetic field was observed. This phenomenon is attributed to the accumulation of interface charges confined in adjacent layers. The magneto-optical measurement demonstrates a magnetic-induced degree of circular polarization in the PL spectra, indicating the Mn incorporation into the QD system. © 2006 American Institute of Physics. [DOI: 10.1063/1.2424654]

Self-assembled diluted magnetic semiconductor<sup>1</sup> (DMS) quantum dots (QDs) are either non-DMS QDs embedded in DMS matrix<sup>2-4</sup> or DMS QDs grown in non-DMS matrix.<sup>5-8</sup> Both types of DMS QDs have potential applications in quantum computation<sup>9</sup> and spintronics devices.<sup>10,11</sup> Several growth techniques were employed to fabricate DMS QDs of high crystal quality. For instance, CdMnSe QDs can be uniformly grown on the Mn-terminated ZnSe surfaces.<sup>5</sup> Also, the growth of CdMnTe QDs can be obtained on Mn-terminated ZnTe surfaces.<sup>6,7</sup>

The above mentioned DMS QD systems all have type-I band alignment. For a QD system of type-II band alignment, the separation of electrons and holes could result in a longer spin relaxation time than those of type-I QDs. Therefore, the type-II QD system could be a potential candidate for magnetic memory due to long spin relaxation time. The reports of the type-II QD structures have so far been mostly concentrated on III-V semiconductor. In this letter, we report the study of DMS ZnMnTe/ZnSe QD structure by molecular beam epitaxy (MBE) and studied the fundamental optical properties by conventional and magneto-PL spectroscopy. Earlier theoretical and experimental studies of ZnTe/ZnSe quantum structures showed that the band alignment of ZnTe/ZnSe is type-II, with the conduction band well in the ZnSe layer and the well in the valence band in the ZnTe layer.<sup>12-16</sup> Because the introduction of Mn further raises the conduction band of ZnTe, the type-II nature of ZnMnTe/ZnSe QD system is expected to be more pronounced than that of ZnTe/ZnSe quantum dots. Holes will be confined in the ZnMnTe QDs and electrons will situate in the ZnSe matrix near QDs by the electron and hole Coulomb attraction. Nonzero circular polarization was observed at zero magnetic field ( $B$ ) for the type-II ZnMnTe QDs. In addition, the circular polarization rate could be manipulated by the applied  $B$ .

The samples studied in this letter were grown on GaAs (100) substrates with an MBE system. The effusion cell temperatures of Zn, Mn, Se, and Te were fixed at 294, 695, 178,

and 310 °C, respectively. The substrate temperature was set at 300 °C. The growth rates for ZnMnTe QDs and ZnSe buffer layers were 0.3 and 0.4 Å/s, respectively. The growth process started with several monolayers of ZnSe by migration enhanced epitaxy, followed by 50 nm of ZnSe by conventional MBE. Immediately after the deposition of ZnSe buffer layer, the alternating supply method of ZnMnTe growth was performed. The alternating supply method for ZnMnTe growth is described as follows: the surface of ZnSe was first exposed to Mn for 5 s, followed by 5 s of ZnTe deposition, with 10 s of interruption between the depositions of Mn and ZnTe. The root mean square roughness of the ZnSe buffer layer, determined from atomic force spectroscopy (AFM), is approximately 0.5 nm. The coverage of the single ZnMnTe QDs layer, grown on the flat ZnSe buffer layer, was varied from 1.8 to 3.0 ML. The transmission electron microscopy (TEM) was performed on a five-layer-ZnMnTe/ZnSe QDs sample with the ZnMnTe coverage of 2.6 ML and ZnSe spacer thickness of 5 nm. A 50 nm ZnSe capping layer was grown on the QDs for optical measurements. A He-Cd 325 nm laser was used to obtain the conventional photoluminescence (PL) spectra, analyzed by a spectrometer equipped with a cooled photomultiplier tube. The magneto-PL spectra were taken in the Faraday geometry. The sample was placed in an optical magnet cryostat and the emitted light was dispersed by a monochromator equipped with multichannel charged coupled device. Excitation source was a 488 nm line of Ar<sup>+</sup> laser. The PL polarization was extracted by using a combination of quarter wave plate and linear polarizer.

Figure 1 shows the cross-sectional TEM of a multilayer ZnMnTe/ZnSe QD structure with 2.6 ML coverage for each ZnMnTe layer and 5 nm for each ZnSe spacer. A schematic drawing to clearly illustrate the TEM picture of Fig. 1 is shown at the right hand side of Fig. 1. Two-dimensional layers associated with ZnMnTe were observed in the cross-sectional TEM, and it is an evidence of the existence of wetting layer. The lateral dot size is about 20 nm and the average height is about 2–3 nm. The planar dot density is

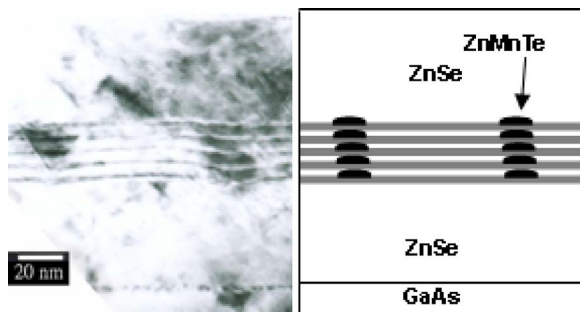


FIG. 1. Cross-sectional TEM of a five-layer QD structure with 2.6 ML of ZnMnTe and 5 nm of ZnSe spacer layers.

estimated to be  $10^9$ – $10^{10}/\text{cm}^2$  from the linear density of Fig. 1. It was confirmed by AFM measurements of the uncapped QDs grown under identical conditions.

Figure 2 shows the low-temperature PL spectra of ZnMnTe QDs with different values of coverage. The sharp PL features near 2.80 eV is attributed to the near band edge emission of the ZnSe matrix. There are mainly two emission bands observed in the PL spectra at the spectral region from 1.8 to 2.6 eV. The lower-energy emission band is due to QD recombination because the corresponding PL peak energy is more sensitive to the change of coverage, compared to that of higher-energy emission band (denoted as *H*). The redshift in energy is attributed to the decrease in the quantum confinement of the holes in the ZnMnTe QDs. It should be noted that the critical coverage for slope change of redshift (near 2.4 ML) is approximately equal to that was observed from the TEM. This indicates a change from two-dimensional wetting layer to three-dimensional ZnMnTe QD formation. Two different redshift slopes were clearly observed for the PL peak energy of the QD emission band, as shown in the inset of Fig. 2. The peak energy decreases rapidly with increasing ZnMnTe coverage when the coverage is less than 2.4 ML. However, above this coverage, the decrease of the peak energy is significantly reduced. This behavior is a characteristic of type-II QDs and is opposite to that of type-I QDs. For

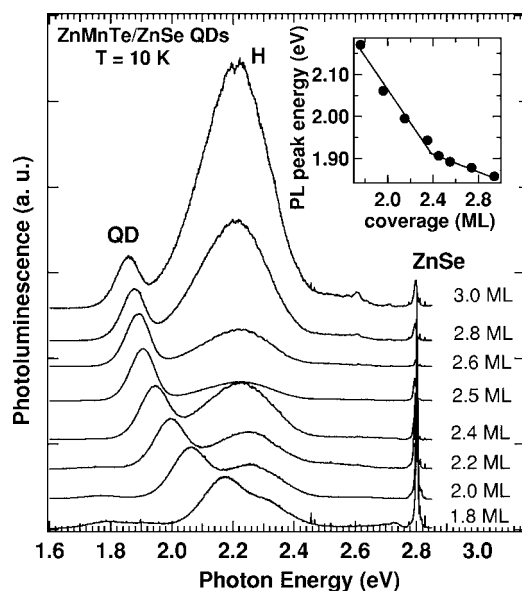


FIG. 2. Low-temperature PL spectra of ZnMnTe QDs with different coverages. The inset shows the PL peak energy of QD as a function of ZnMnTe coverage. The solid line is just a guide for eyes.

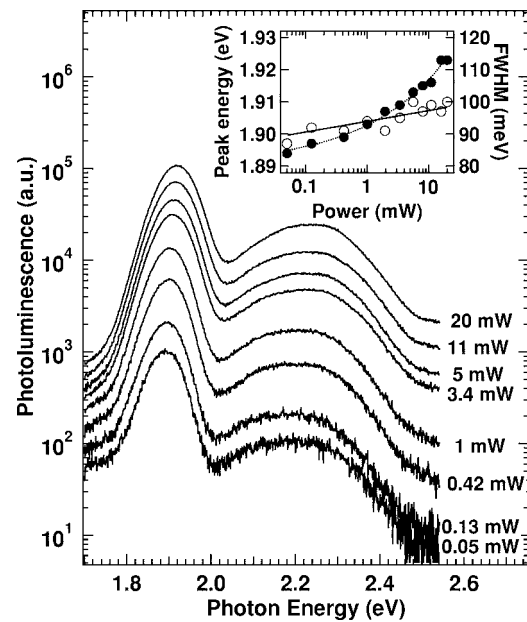


FIG. 3. Power dependence of PL spectra for ZnMnTe QDs with coverage of 2.5 ML. The inset shows the power dependence of PL peak energy (solid circles) and full width at half maximum (open circles). The dashed line is the fit to the PL peak energy, whereas the solid line is just a guide for eyes.

type-I CdSe/ZnSe QDs, for example, the dependence of the PL peak energy on CdSe layer coverage is less when the layer thickness is less than the wetting layer thickness.<sup>17</sup> The type-II nature of the band alignment is also reflected in the observed long radiative recombination time of about 30 ns.

The origin of the *H* emission band is believed to be closely related to the formation of QDs. First, we note that the peak energy of the *H* band slightly redshifts at the critical coverage, but remains almost constant before and after the dot formation. Second, the relative PL intensity of the *H* band, compared to the QD band, increases with increasing coverage, before the critical coverage. It is greatly reduced when the coverage exceeds the critical thickness. The above observation implies that the *H* band emission occurs at regions where dots eventually form, similar to the case of the so-called two-dimensional platelet.<sup>18</sup> As coverage increases from 1.8 to 2.4 ML, the slight redshift in peak energy could be due to the strain effect right before the onset of dot formation. The dramatic reduction of *H*-band intensity can be attributed to the reduction of particular strained structures, when most of them have already evolved into QDs.

Figure 3 shows the PL spectra of ZnMnTe/ZnSe QD with coverage of 2.5 ML as a function of excitation power. There is a significant blueshift for both PL bands as the excitation power increases. This phenomenon, which is usually interpreted as the results of band-bending effect, is characteristic for type-II quantum structures. With higher excitation density, stronger band-bending effect in the heterointerfaces is induced by higher population of spatially confined electron-hole pairs. The quantization energy was shown to increase proportionally with the cube root of the excitation power.<sup>19</sup> This is in good agreement with our experimental data (inset of Fig. 3). We also carefully check the full width at half maximum of the PL peak (see inset) under the excitation power range studied. No obvious broadening was found. This means that the possibility of blueshift due to the band-filling mechanism can be excluded in our case. This

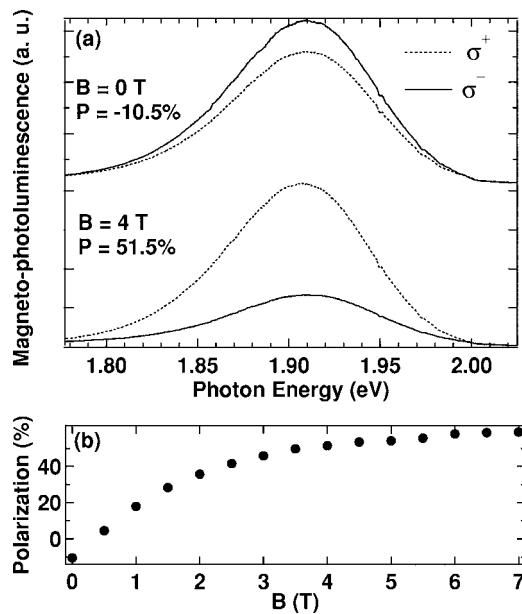


FIG. 4. (a) PL spectra of  $\sigma_+$  (dash line) and  $\sigma_-$  (solid line) polarizations of a 2.6 ML multi-QD layers with 10 nm of spacer layer thickness at  $B=0$  T and  $B=4$  T, (b)  $P$  as a function of  $B$ .

further confirms the type-II nature of emission from the ZnMnTe/ZnSe QDs.

Figure 4(a) shows the PL spectra of  $\sigma_+$  (dash line) and  $\sigma_-$  (solid line) polarizations of a 2.6 ML multi-QD layers with 10 nm of spacer layer thickness at  $B=0$ . The circular polarization degree  $P=(I_+-I_-)/(I_++I_-)$  is  $-10.5\%$  in this case. In this expression,  $I_+$  and  $I_-$  are the integrated of PL intensities of  $\sigma_+$  and  $\sigma_-$  circular polarizations, respectively. The negative  $P$  is unexpected for zero  $B$  because the spin orientation of carriers should be randomized before recombination. This result implies that some built-in  $B$  exists in the multilayer structures. However, the Mn spin alignment is not essential for the built-in  $B$  because the nonzero polarization is less sensitive to thermal energy at least for temperature below 50 K. We believe that this phenomenon is similar to those found in semiconductor heterostructures,<sup>20</sup> where a nonzero spin splitting is possible with a built-in  $B$  induced by the motion of carriers under the presence of nonuniform electric field across the interfaces of ZnMnTe QDs and ZnSe matrices. Therefore, the numbers of spin-oriented carriers involved in radiative recombination is unbalanced, resulting in the negative polarization.

A strong polarization of PL at  $B=4$  T was observed in Fig. 4(a). The observed nonzero polarization is mainly due to the magnetic splitting of the hole spin states in the ZnMnTe QDs. In Fig. 4(b), the circular polarization degree as a function of  $B$ , obtained from low temperature, is plotted. The value of  $P$  increases rapidly at low  $B$  and gradually saturates at high  $B$ . It is a trademark of Brillouin magnetism. The spin polarization was greatly suppressed at temperature above 50 K. Similar results were observable for other DMS QDs.<sup>4,7</sup> Therefore, the incorporation of Mn into our type-II ZnMnTe/ZnSe QD sample was evidenced by the polarization measurement. The Zeeman splitting energy determined by the PL result is 8 meV at  $B=7$  T. According to our growth conditions, the expected Mn concentration in ZnMnTe layer is 11%. Therefore, the Zeeman splitting obtained from the experiment is small than expected. The Zeeman

splitting in a quantum structures depends on the overlap of the exciton wave function and the magnetic moments. In other words, the splitting depends crucially on the Mn distribution, which can be uneven in QDs.<sup>5</sup> Furthermore, the effect of exciton magnetic polaron is enhanced in QDs,<sup>2</sup> and must be accounted for the Zeeman shift. Therefore, the *effective* concentration of Mn incorporation is difficult to be quantitatively determined at this stage. Nevertheless, the data in Fig. 4(b) indicate the formation of magnetic quantum dots, characterized by strong spin-dependent properties in polarization measurement.

In conclusion, MBE-grown type-II DMS ZnMnTe QDs in ZnSe matrix were investigated. The Stranski-Krastanov growth mode was confirmed by cross-sectional TEM. TEM and PL results showed that the critical thickness for dot formation is around 2.4 ML. Our power dependence and time-resolved measurements show that the band alignment in this system is type II. The magnetic field dependent circular polarization study not only shows the existence of Mn in the QDs but also demonstrates the nonzero circular polarization at zero magnetic field, which is the characteristic of type-II ZnMnTe/ZnSe QDs.

This work was supported by MOE-ATU and the National Science Council under the Grant No. of NSC 95-2112-M-009-047.

<sup>1</sup>J. K. Furdyna, J. Appl. Phys. **53**, 7637 (1982).

<sup>2</sup>J. Seufert, G. Bacher, M. Scheibner, A. Forchel, S. Lee, M. Dobrowolska, and J. K. Furdyna, Phys. Rev. Lett. **88**, 027402 (2002).

<sup>3</sup>G. Bacher, H. Schomig, M. K. Welsch, S. Zaitsev, V. D. Kulakovskii, A. Forchel, S. Lee, M. Dobrowolska, J. K. Furdyna, B. Konig, and W. Ossau, Appl. Phys. Lett. **79**, 524 (2001).

<sup>4</sup>E. Oh, K. J. Yee, S. M. Soh, J. U. Lee, J. C. Woo, H. S. Jeon, D. S. Kim, S. Lee, J. K. Furdyna, H. C. Ri, H. S. Chany, and S. H. Park, Appl. Phys. Lett. **83**, 4604 (2003).

<sup>5</sup>L. V. Titova, J. K. Furdyna, M. Dobrowolska, S. Lee, T. Topuria, P. Moeck, and N. D. Browning, Appl. Phys. Lett. **80**, 1237 (2002).

<sup>6</sup>S. Mackowski, T. Gurung, T. A. Nguyen, H. E. Jackson, L. M. Smith, G. Karczewski, and J. Kossut, Appl. Phys. Lett. **84**, 3337 (2004).

<sup>7</sup>S. Mackowski, H. E. Jackson, L. M. Smith, J. Kossut, G. Karczewski, and W. Heiss, Appl. Phys. Lett. **83**, 3575 (2003).

<sup>8</sup>Y. Terai, S. Kuroda, and K. Takita, Appl. Phys. Lett. **76**, 2400 (2000).

<sup>9</sup>D. Loss and D. P. DiVincenzo, Phys. Rev. A **57**, 120 (1998).

<sup>10</sup>P. Recher, E. V. Sukhorukov, and D. Loss, Phys. Rev. Lett. **85**, 1962 (2000).

<sup>11</sup>K. Chang, K. S. Chan, and F. M. Peeters, Phys. Rev. B **71**, 155309 (2005).

<sup>12</sup>Y. Gu, Igor L. Kuskovsky, M. van der Voort, G. F. Neumark, X. Zhou, and M. C. Tamargo, Phys. Rev. B **71**, 045340 (2005).

<sup>13</sup>F. Malonga, D. Bertho, C. Jouanin, and J.-M. Jancu, Phys. Rev. B **52**, 5124 (1995).

<sup>14</sup>C. S. Yang, Y. J. Lai, W. C. Chou, W. K. Chen, M. C. Lee, M. C. Kuo, J. Lee, J. L. Shen, D. J. Jang, and Y. C. Cheng, J. Appl. Phys. **97**, 033514 (2005).

<sup>15</sup>J. Lee, C. S. Yang, C. T. Chang, J. Liu, W. C. Chou, C. M. Lai, G. J. Jan, and Y. S. Huang, Phys. Status Solidi B **241**, 3532 (2004).

<sup>16</sup>T. Y. Lin, D. Y. Lyu, J. Chang, J. L. Shen, and W. C. Chou, Appl. Phys. Lett. **88**, 121917 (2006).

<sup>17</sup>Y. J. Lai, Y. C. Lin, C. B. Fu, C. S. Yang, C. H. Chia, D. S. Chuu, W. K. Chen, M. C. Lee, W. C. Chou, M. C. Kuo, and J. S. Wang, J. Cryst. Growth **282**, 338 (2006).

<sup>18</sup>S. Mackowski, G. Prechtel, W. Heiss, F. V. Kyrychneko, G. Karczewski, and J. Kossut, Phys. Rev. B **69**, 205325 (2004).

<sup>19</sup>N. N. Ledentsov, J. Böhrer, M. Beer, F. Heinrichsdorff, M. Grudmann, D. Bimberg, S. V. Ivanov, B. Ya. Meltser, S. V. Shaposhnikov, I. N. Yassievich, N. N. Faleev, P. S. Kop'ev, and Zh. I. Alferov, Phys. Rev. B **52**, 14058 (1995).

<sup>20</sup>G. Lommer, F. Malcher, and U. Rössler, Phys. Rev. Lett. **60**, 728 (1988).